Stable $M_2AlC(0001)$ surfaces (M = Ti, V and Cr) by first-principles investigation

2008 J. Phys.: Condens. Matter 20 225006

(http://iopscience.iop.org/0953-8984/20/22/225006)

J. Phys.: Condens. Matter **20** (2008) 225006 (11pp) doi:10.1088/0953-8984/20/22/225006

Stable $M_2AlC(0001)$ surfaces (M = Ti, V and Cr) by first-principles investigation

Jiemin Wang[1,2], **Jingyang Wang**[1,3,4] **and Yanchun Zhou**[1]

[1] Shenyang National Laboratory for Materials Science, Institute of Metal Research, Chinese Academy of Sciences, Shenyang 110016, People's Republic of China
[2] Graduate School of Chinese Academy of Sciences, Beijing 100039, People's Republic of China
[3] International Centre for Materials Physics, Institute of Metal Research, Chinese Academy of Sciences, Shenyang 110016, People's Republic of China

E-mail: jywang@imr.ac.cn

Received 10 September 2007, in final form 29 February 2008
Published 16 April 2008
Online at stacks.iop.org/JPhysCM/20/225006

Abstract

We investigated the stable (0001) surfaces of M_2AlC (M = Ti, V and Cr) using the first-principles plane-wave pseudopotential total energy method. Four possible (0001) terminations were considered by breaking the M–Al and M–C bonds. The corresponding surface energies were calculated and compared. The Al- and M(C)-terminated (0001) surfaces demonstrated better stability than the C- and M(Al)- terminated surfaces by their much lower surface energies. In addition, the stability of surfaces was predicted under various chemical environments as a function of chemical potentials. We further investigated the character of surface relaxations. The electronic structures of the stable Al- and M(C)-terminated surfaces were analyzed.

(Some figures in this article are in colour only in the electronic version)

1. Introduction

Recently, a class of nanolaminate ternary ceramics, MAX (where M is an early transition metal, A is an A-group element, and X is carbon and/or nitrogen), has attracted great interest due to excellent properties combining merits of both metals and ceramics, such as a high melting point, low density, high bulk modulus, good thermal and electrical conductivity, excellent thermal shock resistance and high temperature oxidation resistance, damage tolerance, etc [1]. This class of compounds crystallizes in the space group of $P6_3/mmc$. The crystal structures can be described as nanoscale sheets of edge-sharing transition metal carbide or nitride octahedra being weakly bonded with the interleaved planar close packed A-group element layers. In recent years, some MAX phases from the Ti–Si–C [2–7], Ti–Al–C [7–9] and Cr–Al–C [10–12] systems have been deposited as thin films. Investigation of stable surfaces is essential for understanding the growth and nucleation mechanisms for synthesis of MAX-phase thin films. In addition, studies in related fields are important for understanding mechanisms for early stage of oxidation, catalysis, wearing and self-lubricated friction.

Several theoretical models [13–16] have focused on prediction of the stable surface of MAX phases. Since experimental results showed that thin films of the MAX phase typically grew along the [0001] direction [2–12], all these theoretical investigations were focused on (0001) surfaces. Sun and Ahuja calculated the surface energy and surface stress of the $Cr_2AlC(0001)$ surface with the top layer as Al, Cr and C [13]. Music and co-workers have investigated the (0001) surfaces of M_2AC (M = Ti, V and Cr; A = Al, Ga and Ge) [14, 15]. They calculated three different surface terminations, the M, A and C terminations. These works stated that the A termination is the most stable surface. Very recently, the Ti_3AC_2 (A = Si, Al) (0001) surfaces were investigated [16]. In this work, six terminations were considered with respect to cleavage from three kinds of chemical bond in compounds. The authors correlated the surface rumpling with the cleavage energies, discussed the surface stabilities under specific conditions from a thermodynamics point of view and studied the difference in the electronic structure between the surface and bulk form.

[4] Author to whom any correspondence should be addressed.

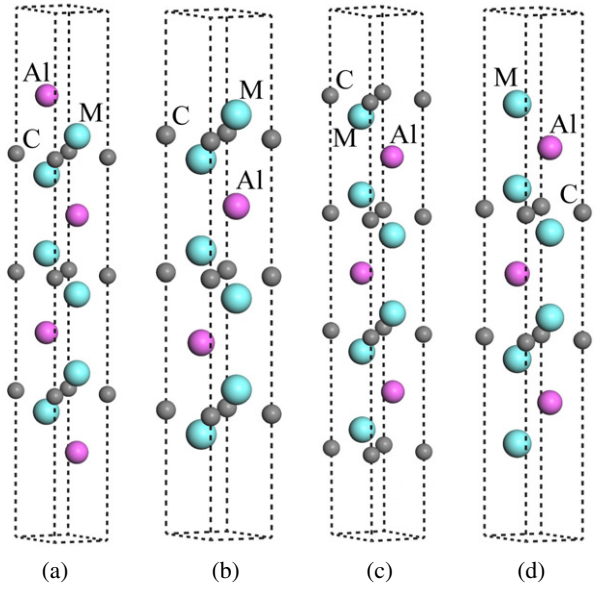

Figure 1. Four possible surface configurations: (a) the Al-terminated surface, (b) the M(C)-terminated surface, (c) the C-terminated surface, (d) the M(Al)-terminated surface.

The present work focused on the M_2AlC (M = Ti, V, and Cr) compounds. These compounds are among the MAX phases most frequently studied in the last decade. They show promising technological applications, such as high temperature structural ceramics. Ti_2AlC showed excellent oxidation resistance by forming a protective Al_2O_3 scale at high temperature [17]. Cr_2AlC also demonstrated good oxidation resistance with its oxidation kinetics following a parabolic rate law [18]. Furthermore, we thought that four different surfaces (one Al termination, one C termination and two M terminations) should be considered and compared by breaking the M–Al and M–C bonds in the M_2AlC compounds (previous investigations focused on three kinds of surfaces [13–15]). In the present paper, two M terminations are represented by M(C)- and M(Al)-terminated surfaces wherein the subsurface atom is given in the brackets. Four considered surface configurations are shown in figure 1. We systemically studied the surface energy, surface stability, surface relaxation and electronic structure of the M_2AlC (M = Ti, V and Cr) (0001) surfaces. The Al- and M(C)-terminated surfaces yield much lower surface energies than C- and M(Al)-terminated surfaces. The stability analysis shows that both the Al- and the M(C)-terminated surfaces can be stable under different chemical environments for Ti_2AlC and V_2AlC, while only the Al-terminated surface is stable under various chemical conditions for Cr_2AlC.

2. Computational method

The present calculation was performed using the CASTEP code, using the plane-wave pseudopotential total energy calculation based on the density functional theory [19]. Within the first-principles calculation, interactions of electrons with ions were represented by a Vanderbilt-type ultrasoft pseudopotential [20] for M (M = Ti, V and Cr), Al and C atoms. The electronic exchange–correlation energy was treated under the generalized gradient approximation (GGA-PW91) [21]. We should note that different exchange–correlation approximations could affect the accuracy of the surface energy. The generalized gradient approximation (GGA) was reported to be less reliable than the local density approximation (LDA). The surface energies calculated by the GGA were often lower than the experimental values [22, 23]. However, when predicting stable surface configurations by comparing surface energy differences, reasonable results can be obtained under the GGA [23–31]. In addition, to continue our early works on the bulk form MAX phase using the GGA method, the present work was accomplished with GGA calculations. Special points sampling integration over the Brillouin zone was employed by using the Monkhorst–Pack method [32].

Before the surface calculation, the bulk equilibrium crystal structures were first obtained. Lattice parameters, including the lattice constant and internal atomic coordinates, were modified to minimize the total energy, interatomic forces and stresses of the unit cell. The Broyden–Fletcher–Goldfarb–Shanno (BFGS) minimization scheme [33] was used in geometrical optimization. The tolerances for geometrical optimization were set as the differences for total energy within 5.0×10^{-6} eV/atom, maximum ionic Hellmann–Feynman force within 0.01 eV $Å^{-1}$, maximum ionic displacement within 5×10^{-4} Å, and maximum stress within 0.02 GPa. The plane-wave basis set cut off was 500 eV, and the k-point mesh was $10 \times 10 \times 2$. Our previous works have shown that the present first-principles calculation scheme was reliable for predicting bulk properties of layered ternary carbides, complex oxides such as $LaPO_4$ monazite, $Y_2Si_2O_7$ and $La_2Zr_2O_7$ pyrochlore [34–39]. Thereafter, full relaxations were performed for all the (1×1) (0001) surface configurations without any symmetric constraint. After relaxation, the interplanar distance between the two central layers changed by less than 0.5% compared with bulk values for all cases. It indicated that the center of the calculated slabs retained the bulk geometry. The plane-wave basis set cut off was 500 eV, and the k-point mesh was $10 \times 10 \times 1$ for surface calculations. We tested the cohesive energy of an 11-layered Ti(C)-terminated surface slab. When increasing the plane-wave cut off to 700 eV and the k-point mesh to $15 \times 15 \times 1$, the cohesive energy differed within 0.003 eV/atom. This indicated that the present calculation parameters were sufficient to describe the surface configurations.

By cleaving from the M–C and M–Al bonds in M_2AlC, four possible terminations can be generated. For example, Al and M(C) terminations are formed after a cleavage from the M–Al bond. Therefore, the (0001) Al- and (0001) M(C)-terminated surfaces are a complementary pair. Similarly, (0001) C- and (0001) M(Al)-terminated surfaces are the other complementary pair. Figure 1 plots the four (0001) surface configurations with Al, M(C), C and M(Al) terminations. All simulations modeled slabs with at least 11 atomic layers. In order to determine the convergence of surface energy with respect to thickness, we tested the cleavage energy created

by breaking the Ti–Al bond in Ti_2AlC by using 7-, 11-, 15- and 19-layered Ti(C)-terminated surface slabs and 9-, 13-, 17- and 21-layered Al-terminated surface slabs. The calculated cleavage energies were 1.993, 1.982, 1.977 and 1.972 J m^{-2}, respectively. The cleavage energy difference between the calculation using 11- and 19-layered Ti(C)-terminated surface slabs was only 0.010 J m^{-2}. This indicated that a slab with more than 11 atomic layers was thick enough. A vacuum of 10 Å thickness was selected to avoid unphysical interactions between two adjacent surfaces.

The calculations of the projected density of states were performed using a projection of the plane-wave electronic states onto a localized linear combination of atomic orbitals (LCAO) basis set. In the present calculation, the LCAO basis set was the atomic pseudo-orbitals corresponding to the closed valence shell containing the valence electrons. The s, p valence orbitals of C, as well as the s, p orbitals of Al and the s, p and d orbitals of M were included in the calculation of the partial density of states (PDOS). Since M_2AlC compounds are metallic systems, partial occupancies were introduced to eliminate discontinuous changes in the total energy created when energy bands crossed the Fermi level during self-consistent electronic minimization. Twelve additional empty bands were included in the electronic minimization, and we used the Gaussian smearing scheme with a smearing width of 0.1 eV.

3. Results and discussion

3.1. Surface energy

Surface energy is a fundamental parameter which governs the global thermodynamically stable surface configurations. In the present work, surface energy calculations were carried out under an approximation that has been accurately used for ternary ceramics [26, 40, 41]. The process of surface forming can be separated into two steps. In the first step, the surface configuration retains the unrelaxed structure of the bulk state, and the system gains energy from rigid cleavage. In the second step, atomic relaxation is considered to decrease the surface stress. Under the framework of this approximation, the surface energy is calculated in two parts, cleavage energy and relaxation energy. Two complementary surfaces are created when a crystal cleaves in certain atomic plane. The approximation assumes that the cleavage energy is distributed equally to the two complementary surfaces. For $M_2AlC(0001)$ surfaces, the Al- and M(C)-terminated surfaces share the same cleavage energy, and so do the M(Al)- and C-terminated surface pair. The surface energies of Al- and C-terminated surfaces are calculated using 13-layered slabs; and 11-layered slabs are used for calculating the M(C)- and M(Al)-terminated surface energies. The chemical compositions of all the used slabs with the same terminations on both ends deviate from the stoichiometry of bulk material. But when two complementary slabs (Al and M(C), or C and M(Al)) are put together, the composite contains three stoichiometric bulk unit cells. The cleavage energy can be expressed as:

$$E_{\text{cleav}}^{\text{M-Al}} = (E_{\text{unrelax}}^{\text{Al}} + E_{\text{unrelax}}^{\text{M(C)}} - 3E_{\text{bulk}})/4A; \quad (1)$$

$$E_{\text{cleav}}^{\text{M-C}} = (E_{\text{unrelax}}^{\text{C}} + E_{\text{unrelax}}^{\text{M(Al)}} - 3E_{\text{bulk}})/4A \quad (2)$$

where $E_{\text{cleav}}^{\text{M-Al}}$ and $E_{\text{cleav}}^{\text{M-C}}$ are the cleavage energies for breaking the M–Al and M–C bonds, respectively. $E_{\text{unrelax}}^{\text{Al}}$, $E_{\text{unrelax}}^{\text{M(C)}}$, $E_{\text{unrelax}}^{\text{C}}$ and $E_{\text{unrelax}}^{\text{M(Al)}}$ are the total energies without structural relaxations, and E_{bulk} is the total energy of the bulk compound. A represents the section area of a unit cell. The factor of 4 before A originates from the fact that two slabs have four surfaces. Next, we calculated the relaxation energies after performing structural relaxation on each slab:

$$E_{\text{R}}^{\text{T}} = (E_{\text{unrelax}}^{\text{T}} - E_{\text{relax.}}^{\text{T}})/2A. \quad (3)$$

The superscript T (T = Al, M(C), C and M(Al)) represents the different terminations of the slab. E_{R}^{T} represents the relaxation energy of the T-terminated surface. $E_{\text{unrelax}}^{\text{T}}$ is the total energy before relaxation, and $E_{\text{relax.}}^{\text{T}}$ is the energy of the slab after relaxation. A represents the section area of a unit cell. The factor of 2 before A comes from the fact that one slab has two surfaces. Finally, the surface energy is calculated by subtracting the relaxation energy from the cleavage energy:

$$E_{\text{S}}^{\text{Al}} = E_{\text{cleav}}^{\text{M-Al}} - E_{\text{R}}^{\text{Al}}, \quad (4a)$$

$$E_{\text{S}}^{\text{M(C)}} = E_{\text{cleav}}^{\text{M-Al}} - E_{\text{R}}^{\text{M(C)}}, \quad (4b)$$

$$E_{\text{S}}^{\text{M(Al)}} = E_{\text{cleav}}^{\text{M-C}} - E_{\text{R}}^{\text{M(Al)}}, \quad (4c)$$

$$E_{\text{S}}^{\text{C}} = E_{\text{cleav}}^{\text{M-C}} - E_{\text{R}}^{\text{C}}. \quad (4d)$$

Calculated surface energies are listed in table 1, together with the cleavage and relaxation energies. As shown in the table, the cleavage energy has a dominant contribution to the surface energy. For Al- and M(Al)-terminated surfaces, the ratio of relaxation energy to cleavage energy is less than 0.8%; and the ratio is less than 3.6% for M(C)-terminated surfaces. The C-terminated surfaces have relatively larger ratio varying between 12% and 32%. The cleavage energy for breaking the M–C bond is about 3.3–4.3 J m^{-2} larger than that for breaking the M–Al bond. This indicates that the M(Al)- and C-terminated surfaces are more difficult to form than the Al- and M(C)-terminated surfaces. The present surface energies of (0001) Al-terminated are well consistent with the value reported by Music *et al* [14, 15]. The deviation is less than 0.12 J m^{-2}. The surface energies of (0001) M(Al)-terminated surfaces are overestimated and the surface energies of (0001) C-terminated surfaces are slightly underestimated. It is clear that the deviations are almost the same for the three compounds, suggesting a systematic error of surface energy deduced from different calculation methods.

For all three compounds the calculated surface energies of Al- and M(C)- terminated surfaces are very close and much smaller than those of C- and M(Al)-terminated surfaces. In Ti_2AlC, the Al- and Ti(C)-terminated surface energies are 1.967 and 1.978 J m^{-2}; while the surface energies of C and Ti(Al) terminations are 4.266 and 6.188 J m^{-2}. Similarly for V_2AlC, the Al- and V(C)-terminated surface energies are 2.428 and 2.346 J m^{-2}, respectively, and the C- and V(Al)-terminated surface energies are 5.002 and 6.003 J m^{-2}, respectively. The same tendency also appears for Cr_2AlC: the Al- and

Table 1. The calculated cleavage energies (in J m^{-2}), relaxation energies (in J m^{-2}) and surface energies (in J m^{-2}) for M_2AlC (M = Ti, V and Cr).

					Surface energy	
	Bond	Cleavage energy	Terminated surface	Relaxation energy	This work	[14]
Ti_2AlC	Ti–Al	1.982	Al	0.015	1.967	1.974
			Ti(C)	0.004	1.978	
	Ti–C	6.234	C	1.968	4.266	5.262
			Ti(Al)	0.046	6.188	5.264
V_2AlC	V–Al	2.432	Al	0.004	2.428	2.312
			V(C)	0.086	2.346	
	V–C	6.032	C	1.030	5.002	5.402
			V(Al)	0.029	6.003	5.403
Cr_2AlC	Cr–Al	2.481	Al	0.002	2.479	2.409
			Cr(C)	0.061	2.420	
	Cr–C	5.806	C	0.713	5.093	5.358
			Cr(Al)	0.036	5.770	5.357

Cr(C)-terminated surface energies, 2.479 and 2.420 J m^{-2}, respectively, are smaller than the C- and Cr(Al)-terminated surface energies, 5.093 and 5.770 J m^{-2}. This suggests that the Al- and M(C)-terminated surfaces are more stable than the C- and M(Al)-terminated surfaces. Because of the close values for the Al- and M(C)-terminated surfaces, both surfaces are energetically favorable.

3.2. Surface stability

When a material is in an open system and can exchange atoms with its surroundings, the surface stability will be affected by the chemical environment. The surface grand potential (SGP) should be considered to analyze the surface stability. The SGP is the excess Gibbs free energy of the surface in contact with various matter reservoirs as a function of the chemical potentials of different atomic species. This method has been extensively used for studying surface stability [26–28, 42–46].

The surface grand potential per unit cell area, Ω^{T}, corresponding to the T termination is defined as:

$$\Omega^{\mathrm{T}} = \tfrac{1}{2}[E^{\mathrm{T}}_{\mathrm{relax}} - N_{\mathrm{M}}\mu_{\mathrm{M}} - N_{\mathrm{Al}}\mu_{\mathrm{Al}} - N_{\mathrm{C}}\mu_{\mathrm{C}}] \tag{5}$$

where $E^{\mathrm{T}}_{\mathrm{relax}}$ denotes the slab energy of T (T = Al, M(C), C and M(Al)) termination, N_{M}, N_{Al} and N_{C} are the atomic number of M (M = Ti, V and Cr), Al, and C, respectively, in the T termination slab. μ_{M}, μ_{Al} and μ_{C} represent the chemical potential of M (M = Ti, V and Cr), Al and C atomic species. Since the surface is in equilibrium with the bulk M_2AlC, the following equation is satisfied:

$$2\mu_{\mathrm{M}} + \mu_{\mathrm{Al}} + \mu_{\mathrm{C}} = E^{\mathrm{Bulk}}_{\mathrm{M_2AlC}}. \tag{6}$$

Substituting equation (6) to (5), the expression for SGP can be rewritten as:

$$\Omega^{\mathrm{T}} = \frac{1}{2}\left[E^{\mathrm{T}}_{\mathrm{relax}} - \frac{N_{\mathrm{M}}}{2}E^{\mathrm{Bulk}}_{\mathrm{M_2AlC}} + \left(\frac{N_{\mathrm{M}}}{2} - N_{\mathrm{Al}}\right)\mu_{\mathrm{Al}} + \left(\frac{N_{\mathrm{M}}}{2} - N_{\mathrm{C}}\right)\mu_{\mathrm{C}}\right]. \tag{7}$$

If we know the upper and lower boundary values of the three chemical potentials, we can deduce the accessible range of each termination.

Introducing the variation chemical potentials with respect to the reference phases,

$$\Delta\mu_{\mathrm{M}} = \mu_{\mathrm{M}} - E^{\mathrm{Bulk}}_{\mathrm{M}}, \tag{8a}$$

$$\Delta\mu_{\mathrm{Al}} = \mu_{\mathrm{Al}} - E^{\mathrm{Bulk}}_{\mathrm{Al}}, \tag{8b}$$

$$\Delta\mu_{\mathrm{C}} = \mu_{\mathrm{C}} - E^{\mathrm{Bulk}}_{\mathrm{C}}. \tag{8c}$$

Here the choosen reference phases are hexagonal close packed Ti, body centered cubic V and Cr, face centered cubic Al, and graphite. The equations (5) and (6) can be rewritten as:

$$\Omega^{\mathrm{T}} = \Phi^{\mathrm{T}} + \frac{1}{2}\left[\left(\frac{N_{\mathrm{M}}}{2} - N_{\mathrm{Al}}\right)\Delta\mu_{\mathrm{Al}} + \left(\frac{N_{\mathrm{M}}}{2} - N_{\mathrm{C}}\right)\Delta\mu_{\mathrm{C}}\right], \tag{9}$$

$$\Phi^{\mathrm{T}} = \frac{1}{2}\left[E^{\mathrm{T}}_{\mathrm{relax}} - \frac{N_{\mathrm{M}}}{2}E^{\mathrm{Bulk}}_{\mathrm{M_2AlC}} + \left(\frac{N_{\mathrm{M}}}{2} - N_{\mathrm{Al}}\right)E^{\mathrm{Bulk}}_{\mathrm{Al}} + \left(\frac{N_{\mathrm{M}}}{2} - N_{\mathrm{C}}\right)E^{\mathrm{Bulk}}_{\mathrm{C}}\right], \tag{10}$$

$$2\Delta\mu_{\mathrm{M}} + \Delta\mu_{\mathrm{Al}} + \Delta\mu_{\mathrm{C}} = E^{f}_{\mathrm{M_2AlC}}. \tag{11}$$

Constants Φ^{T} and the values of (N_{M}/2-N_{Al}) and (N_{M}/2-N_{C}) for each termination of M_2AlC are given in table 2. The formation energy is defined as:

$$E^{f}_{\mathrm{M_2AlC}} = E^{\mathrm{Bulk}}_{\mathrm{M_2AlC}} - 2E^{\mathrm{Bulk}}_{\mathrm{M}} - E^{\mathrm{Bulk}}_{\mathrm{Al}} - E^{\mathrm{Bulk}}_{\mathrm{C}}. \tag{12}$$

The calculated values of $E^{f}_{\mathrm{Ti_2AlC}} = -2.76$ eV, $E^{f}_{\mathrm{V_2AlC}} = -2.03$ eV, and $E^{f}_{\mathrm{Cr_2AlC}} = -0.76$ eV.

Considering the stability condition, the variation chemical potentials must be negative. The reason is that the chemical potential of each atomic species must be lower than the energy of the atom in the stable bulk phase, otherwise the stable bulk phase will precipitate from the compound. So, the following upper boundaries can be introduced:

Table 2. Constants Φ^{T} and the values of $(N_M/2 - N_{Al})$ and $(N_M/2 - N_C)$ defined in equations (9) and (10) for each termination of M_2AlC (M = Ti, V and Cr).

			Φ^{T} (eV/unit)		
Termination	$(N_M/2 - N_{Al})$	$(N_M/2 - N_C)$	Ti_2AlC	V_2AlC	Cr_2AlC
Al	−1	0	0.61	0.63	0.61
M(C)	1	0	1.40	1.53	1.50
C	0	−1	2.96	2.59	2.45
M(Al)	0	1	2.31	2.39	2.23

$$\Delta\mu_M < 0, \tag{13a}$$

$$\Delta\mu_{Al} < 0, \tag{13b}$$

$$\Delta\mu_C < 0. \tag{13c}$$

Combining the upper boundaries with equation (11), we can get the lower boundaries:

$$\Delta\mu_M > \tfrac{1}{2}E^f_{M_2AlC}, \tag{14a}$$

$$\Delta\mu_{Al} > E^f_{M_2AlC}, \tag{14b}$$

$$\Delta\mu_C > E^f_{M_2AlC}. \tag{14c}$$

Besides the simple substance, some related binary carbides often appear during the synthesizing or oxidizing processes. It is significant to consider the precipitation of these binary phases. It will bring some more boundaries between the above-mentioned upper and lower boundaries and decrease the accessible range of chemical potentials. We considered TiC for Ti_2AlC, VC for V_2AlC, Cr_7C_3 for Cr_2AlC, and Al_4C_3 for all three compounds. The following boundary conditions can be obtained, for Ti_2AlC:

$$\Delta\mu_{Ti} + \Delta\mu_C < E^f_{TiC}, \tag{15a}$$

$$4\Delta\mu_{Al} + 3\Delta\mu_C < E^f_{Al_4C_3}; \tag{15b}$$

for V_2AlC:

$$\Delta\mu_V + \Delta\mu_C < E^f_{VC}, \tag{16a}$$

$$4\Delta\mu_{Al} + 3\Delta\mu_C < E^f_{Al_4C_3}; \tag{16b}$$

for Cr_2AlC:

$$7\Delta\mu_{Cr} + 3\Delta\mu_C < E^f_{Cr_7C_3}, \tag{17a}$$

$$4\Delta\mu_{Al} + 3\Delta\mu_C < E^f_{Al_4C_3} \tag{17b}$$

where the formation energies are defined as:

$$E^f_{TiC} = E^{Bulk}_{TiC} - E^{Bulk}_{Ti} - E^{Bulk}_{C}, \tag{18}$$

$$E^f_{VC} = E^{Bulk}_{VC} - E^{Bulk}_{V} - E^{Bulk}_{C}, \tag{19}$$

$$E^f_{Cr_7C_3} = E^{Bulk}_{Cr_7C_3} - 7E^{Bulk}_{Cr} - 3E^{Bulk}_{C}, \tag{20}$$

$$E^f_{Al_4C_3} = E^{Bulk}_{Al_4C_3} - 4E^{Bulk}_{Al} - 3E^{Bulk}_{C}. \tag{21}$$

The calculated formation energies of TiC, VC, Cr_7C_3 and Al_4C_3 are −1.56 eV, −0.74 eV, −0.84 eV and −1.54 eV, respectively.

In the accessible ranges of the chemical potentials, the most stable termination has the smallest value of surface grand potential. The boundaries between stable regions of different terminations can be deduced by the solution of following equations:

$$\Omega^{Al} = \Omega^{M(C)}, \tag{22a}$$

$$\Omega^{Al} = \Omega^{C}, \tag{22b}$$

$$\Omega^{Al} = \Omega^{M(Al)}, \tag{22c}$$

$$\Omega^{M(C)} = \Omega^{C}, \tag{22d}$$

$$\Omega^{M(C)} = \Omega^{M(Al)}, \tag{22e}$$

$$\Omega^{C} = \Omega^{M(Al)}. \tag{22f}$$

In addition, the surface grand potential must be positive. Otherwise, the surface is more stable than the bulk. So, the following boundary conditions should be added:

$$\Omega^{Al} > 0, \tag{23a}$$

$$\Omega^{M(C)} > 0, \tag{23b}$$

$$\Omega^{C} > 0, \tag{23c}$$

$$\Omega^{M(Al)} > 0. \tag{23d}$$

Figure 2 shows the stability diagrams of M_2AlC (M = Ti, V and Cr) (0001) surfaces by summarizing all the boundary conditions. Since equation (11) is always satisfied, we can use ternary coordinates which are very similar to the coordinates employed in the ternary phase diagram. There are three kinds of line in the figure. The spontaneous surface formation lines of equations (23) are plotted by the thin solid lines. If crossing these lines, the surface will form spontaneously and the crystal will be destroyed. The dotted lines are the boundaries between stable regions of different terminations. They are the solutions of equations (22). The boundary lines separate the whole range into four parts which are distinguished by different fill patterns. Each one represents one certain termination which is most stable in the corresponding area. The thick solid lines are the precipitation lines of the simple substances corresponding to equations (13) and (14). The dash dotted lines are the precipitation lines of binary carbides obtained by equations (15)–(17) for Ti_2AlC, V_2AlC and Cr_2AlC, respectively. The corresponding materials will precipitate from M_2AlC if the chemical potentials cross these precipitation lines. This will cause defect formation in M_2AlC crystals because of the deviation from stoichiometric composition. The perfect crystal of M_2AlC without defects can exist in the stable area which is confined by the spontaneous surface formation lines and the precipitation lines. For Ti_2AlC, the stable area is confined by the Al, Ti, TiC and Al_4C_3 precipitation lines.

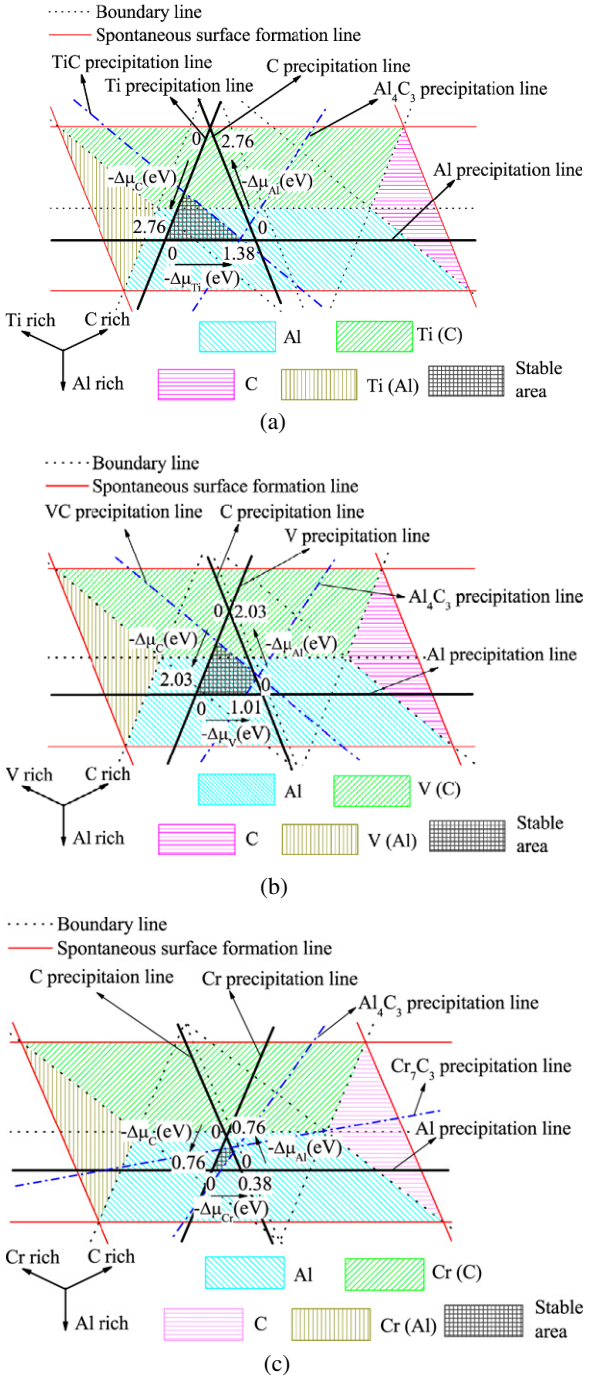

Figure 2. Stability diagrams of M_2AlC (M = Ti, V and Cr) (0001) surfaces: (a) for Ti_2AlC, (b) for V_2AlC and (c) for Cr_2AlC. The surface stability is represented by ternary coordinates of $\Delta\mu_M$, $\Delta\mu_{Al}$ and $\Delta\mu_C$. The thin solid lines are the spontaneous surface formation lines. The dotted lines are the boundaries between stable regions of different terminations. The thick solid lines are the simple substances precipitation lines. The dash dotted lines are the precipitation lines of binary carbides.

For V_2AlC, all the precipitation lines, Al, V, C, VC and Al_4C_3, are boundaries of the stable area. Similarly for V_2AlC, the stable area of Cr_2AlC is surrounded by all the precipitation lines, Al, Cr, C, Cr_7C_3 and Al_4C_3. Of most interest, the stable area of Ti_2AlC and V_2AlC is covered by both Al- and M(C)-terminated surface stable regions, while for Cr_2AlC, the stable area only contains an Al-terminated surface stable region. This suggests that both the Al and M(C) terminations can be stable for Ti_2AlC and V_2AlC under different conditions, while only the Al-terminated (0001) surface is stable for Cr_2AlC.

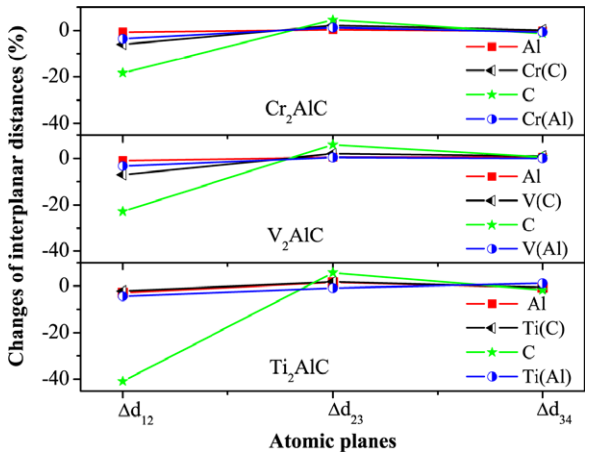

Figure 3. The changes of inter-planar distance in $M_2AlC(0001)$ surfaces. Δ_{ij} (i = 1–3, and j = 2–4) represents the inter-planar distance between layers i and j.

3.3. Surface relaxations

Surface relaxation is an important characteristic of M_2AlC surfaces. For the M(C)-terminated surface, the relaxation energies vary in the order V_2AlC > Cr_2AlC > Ti_2AlC; for relaxation energies of the other three surfaces, the values of V_2AlC and Cr_2AlC are smaller than those of Ti_2AlC. The surface relaxations exhibit close correlation with the magnitude of the corresponding relaxation energies. We further studied the changes of inter-planar distances, which are caused by decrements of coordination number for atoms in the surface layer [42]. After cleavage along a certain atomic plane, the equilibrium of bonding coordination for the surface atom is broken; and meanwhile, the redistribution of surface electrons can strengthen the coupling between the surface and subsurface layer. As a result, the surface layer should relax inward, while the subsurface layer will relax outward. The distortion spreads into the inner part with a rapid decreasing magnitude. Therefore, the inter-planar distance between the first two layers changes significantly and represents predominantly the surface relaxation.

The $Cr_2AlC(0001)$ surface relaxation has been investigated in [13]. The outward relaxation of the subsurface atomic layer was much less than the inward relaxation of the top surface layer. And the top surface layer of the (0001) C-terminated surface exhibited the largest inward relaxation. Following a similar method, we calculated the relaxations of the top three atomic layers for four (0001) surfaces of M_2AlC (M = Ti, V and Cr). Figure 3 shows the changes of inter-planar distance in each termination of M_2AlC (0001) surfaces. Three characteristics are identified for surface relaxation. First, for all the surfaces, the top layer atomic plane relaxes inwardly and the

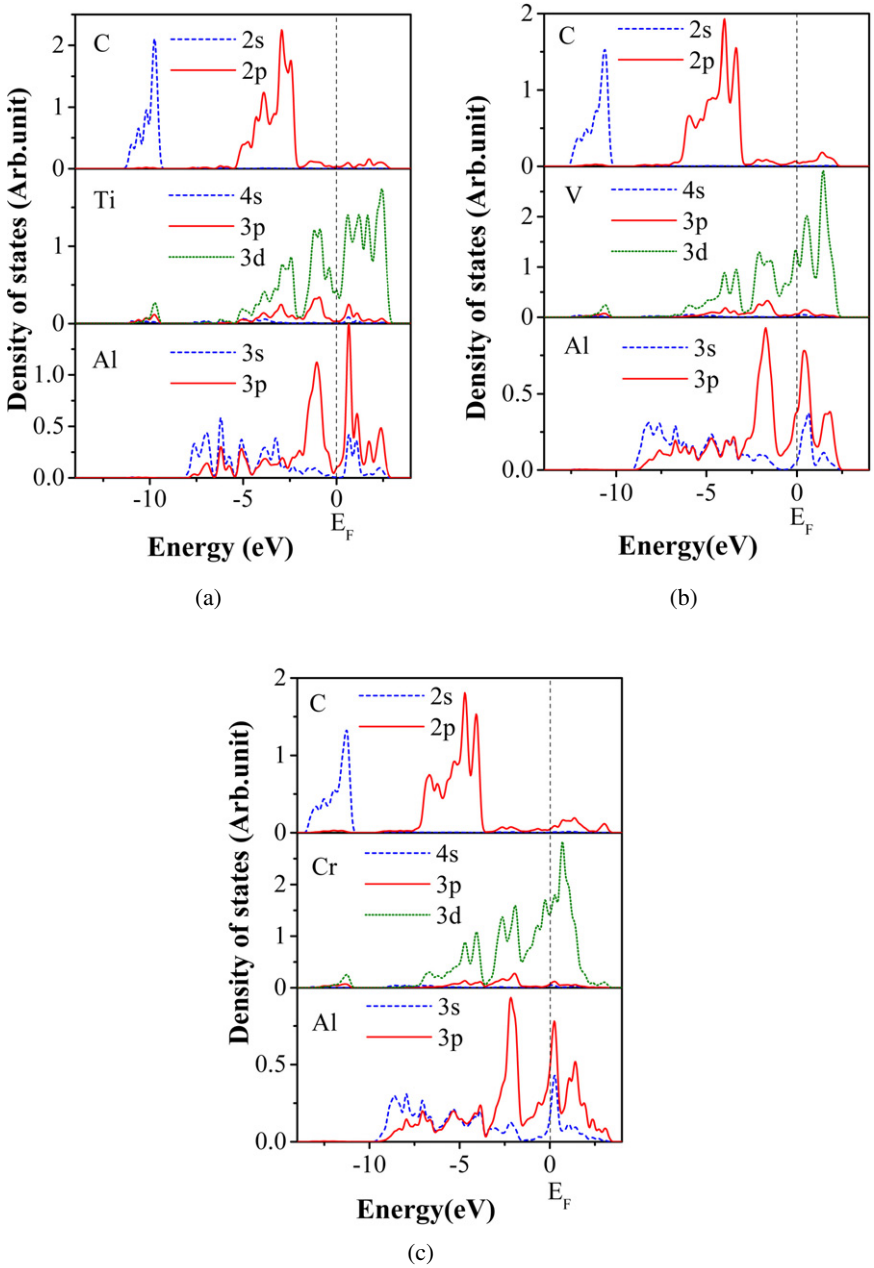

Figure 4. The PDOS of the top three layers of Al-terminated (0001) surfaces for (a) Ti_2AlC, (b) V_2AlC, (c) Cr_2AlC.

subsurface layer moves outward. This indicates that the inter-planar distance of the top two layers is less than the value in the bulk material. Second, relaxation decreases from the top layer to the third layer for all the (0001) surfaces. Below the third layer, the inter-planar distance is almost the same as in bulk material. Third, the C-terminated surface shows the largest relaxation in the top layer for Ti_2AlC, V_2AlC and Cr_2AlC. This agrees with the theoretical analysis in previous works [13].

In addition, the same trends for changes of the surface relaxation and relaxation energy have been found. For Al- and C-terminated surfaces, the surface relaxations and relaxation energies decrease in the order of $Ti_2AlC > V_2AlC > Cr_2AlC$. For M(C) termination, the V(C)-terminated surface relaxation of V_2AlC is the largest (-7.03%); the Ti(C)-terminated surface relaxation of Ti_2AlC is the smallest (-2.23%); and the Cr(C)-terminated surface relaxation of Cr_2AlC is between them (-5.90%). The corresponding relaxation energies are 0.086 J m^{-2}, 0.004 J m^{-2} and 0.061 J m^{-2} for V_2AlC, Ti_2AlC and Cr_2AlC, respectively. For M(Al) termination, surface relaxation increases from -3.34% of V_2AlC to -3.54% of Cr_2AlC, and then to -4.40% of Ti_2AlC; and the surface relaxation energies are 0.029 J m^{-2} of V_2AlC, 0.036 J m^{-2} of Cr_2AlC and 0.046 J m^{-2} of Ti_2AlC.

3.4. Electronic structure analysis

3.4.1. Bulk M_2AlC. The character of the atomic bonding has been clearly demonstrated by the projected electronic density of states (PDOS) in previous studies [47–49]. For Ti_2AlC, the deepest core states between -11.11 and -9.53 eV

correspond to the C 2s orbitals. The Ti 3d–C 2p hybridization locates from −5.21 to −2.32 eV below the Fermi level. The Ti 3d–Al 3p bonding orbitals appear between −2.41 and 0.84 eV. Therefore, the Ti–Al bond is weaker than the Ti–C bond according to its higher energy range. The states near and above the Fermi level are attributed to metal–metal d–d bonding and antibondings. The pseudogap which separates the bonding and antibonding groups of Ti 3d–Al 3p hybridization approximately locates at the Fermi level. The PDOS of V_2AlC and Cr_2AlC are rather similar to that of Ti_2AlC except that bonding states shift downward away from the Fermi level after the substitution of Ti by V and further by Cr. The pseudogap which separates the bonding and antibonding groups of Cr 3d–Al 3p hybridization moves to −1.5 eV for Cr_2AlC. Wang *et al* stated that the Ti–Al d–p bonding orbitals were not fully occupied and can be filled with more electrons in Ti_2AlC; the V–Al d–p bonding orbitals were nearly fully occupied; while for Cr_2AlC, the Cr–Al d–p bonding orbitals were completely occupied and excessive electrons only filled Cr–Cr d–d metallic bonding [50].

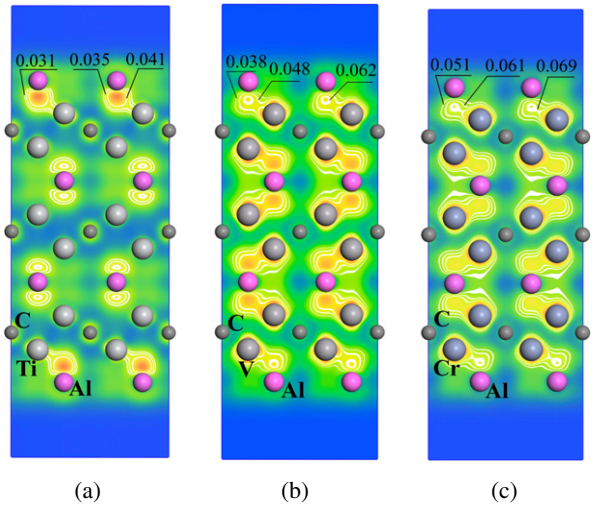

Figure 5. Valence electron density of Al-terminated (0001) surfaces. The plots are in the $(11\bar{2}0)$ plane. Panel (a) includes the energy range between −2.45 and −0.87 eV in Ti_2AlC. Panel (b) covers −3.15 through −0.35 eV in V_2AlC. Panel (c) ranges from −3.57 to −1.11 eV in Cr_2AlC.

3.4.2. Al-terminated surface. According to the electronic structure of the bulk form, the M–C bond is stronger than the M–Al bond. So, the cleavage energy to break M–C bond is larger than that for breaking the M–Al bond. The Al- and M(C)-terminated(0001) surfaces possess smaller surface energies than the other surfaces. Figure 4 plots the PDOS of Al-terminated surfaces of M_2AlC (M = Ti, V and Cr). The most significant change from the bulk PDOS is that the peak of M–Al d–p antibonding appears above the pseudogap. Since the pseudogap in Ti_2AlC locates just at the Fermi level, the Ti–Al d–p antibonding orbitals are unoccupied. While for V_2AlC and Cr_2AlC, the pseudogaps locate below the Fermi level, and the antibonding peaks run across the Fermi level. This indicates that some of the M–Al d–p antibonding orbitals are filled in the surfaces of V_2AlC and Cr_2AlC. So, the Al-terminated surfaces of V_2AlC and Cr_2AlC are expected to possess higher surface energy because of occupation of antibonding orbitals. This is consistent with the calculation results.

To learn more details about surface atomic bonding and electron redistribution, we checked the valence electron density of the Al-terminated surfaces. The Al-terminated surface is generated by breaking the M–Al bond and leaving the Al atoms on the top surface of M_2AlC. Therefore, 3p valence electrons of the Al atom in the broken Ti–Al bond will redistribute in the surface area. There are two possible ways that the 3p electrons redistribute: (i) occupation of states in an unbroken Ti–Al bond in the surface area; and (ii) filling the surface Al–Al bond. Figure 5 shows the valence electron density of states in the energy range from −2.45 and −0.87 eV in Ti_2AlC, −3.15 through −0.35 eV in V_2AlC, and from −3.57 to −1.11 eV in Cr_2AlC. These energy ranges are chosen for covering the surface M–Al bonding states. As shown in figure 5(a), the electron density of Ti–Al bonding in the area of the surface is obviously higher than that in the inner area. Since the Ti–Al bond is not fully filled in bulk Ti_2AlC, as discussed before, the redistributed 3p electrons prefer to occupy Ti–Al bonding states first. Thereafter, the electron density of the Ti–Al bond in the surface area is higher than that in the inner area, and the Ti–Al bond is strengthened. For the case of V_2AlC and Cr_2AlC, different occupations of 3p electrons are observed. As shown in figures 5(b) and (c), no further occupation of the M–Al bond in the surface area is identified for V_2AlC and Cr_2AlC after redistribution of Al 3p electrons. This is reasonable since the V–Al d–p bonds are almost fully occupied and the Cr–Al d–p bonds are already completely filled in bulk form. Most of the redistributed Al 3p electrons fill the V–Al antibonding orbitals in the surface area for V_2AlC. For Cr_2AlC, the redistributed Al 3p electrons will not occupy the saturated Cr–Al d–p bonding orbitals but in turn fill the Cr–Al antibonding orbitals in the surface area. In addition, the V–Al and Cr–Al bonds in the surface area are not strengthened as the Ti–Al bond because there is no further occupation of bonding orbitals. As a result, relaxations of Al-terminated surfaces are smaller in V_2AlC and Cr_2AlC than in Ti_2AlC. This analysis agrees with the results of surface relaxation calculations.

3.4.3. M(C)-terminated surface. M(C)-terminated surfaces are generated by breaking the M–Al bond and leaving the M atoms on the top surface. The 3d valence electrons may redistribute in two ways: occupation of M–M d–d metallic bonding and filling the M–C bonding orbitals in the subsurface. However, the M–C bonding orbitals are already fully occupied in M_2AlC, and only the M–M d–d metallic bonding orbitals can be filled. Figure 6 shows the PDOS of M(C)-terminated surfaces of M_2AlC (M = Ti, V and Cr). Some peaks appear for the first time near the Fermi level which originates from M–M d–d metallic bonding. When a Ti atom is substituted by V and Cr, the M–Al d–p bonding states move to lower energy ranges. The electrons of surface M atoms needs more energy to jump from M–Al bonding orbitals to surface M–M metallic bonding orbitals when breaking surface M–Al bonds.

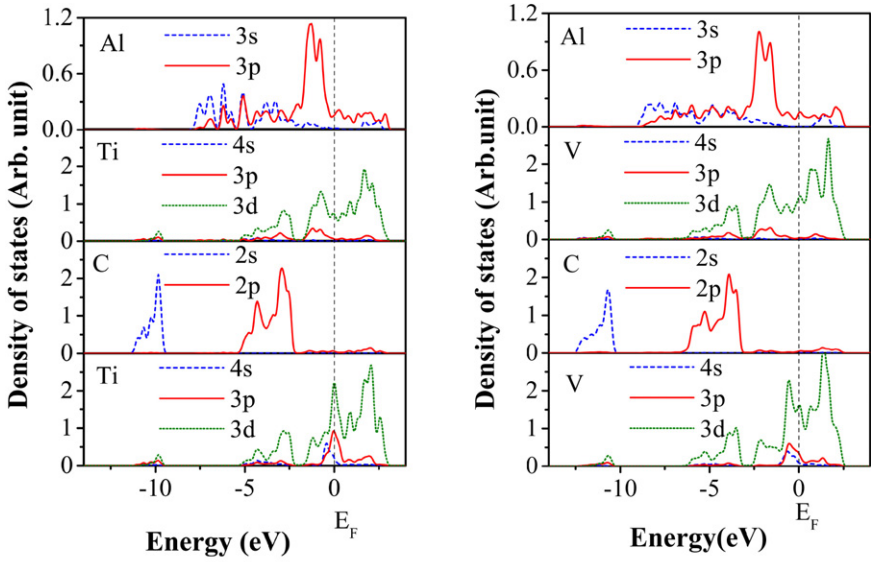

Figure 6. PDOS of the top four layers of M(C)-terminated (0001) surfaces for (a) Ti_2AlC, (b) V_2AlC and (c) Cr_2AlC.

As a result, the surface energy of V(C)- and Cr(C)-terminated surfaces is higher than that of a Ti(C)-terminated surface. We further analyzed the electron densities shown in figures 7(a)–(c) for the distribute of states in the energy ranges from −2.40 to 0.73 eV for Ti_2AlC, −3.18 to −0.02 eV for V_2AlC, and −3.55 to −0.52 eV for Cr_2AlC. In the inner area, the valence electrons of M atoms distribute between M and Al atoms, forming M–Al bonds. While in the surface layer, after breaking M–Al bonds, the electrons of M atoms redistribute between M atoms in the surface layer. This suggests that the 3d valence electrons of surface M atoms redistribute and occupy the M–M d–d metallic bonding.

In brief, the electronic structure characteristics of stable Al- and M(C)- terminated surfaces are summarized as follows. In Al-terminated surfaces, the redistributed Al 3p electrons fill the Ti–Al bonding states and strengthen the Ti–Al bond; while the redistributed Al 3p electrons will occupy V–Al and Cr–Al antibonding orbitals in the surface area, which increases the surface energy. For the M(C)-terminated surface, the redistributed M 3d electrons prefer to occupy the M–M d–d metallic bonding states for M_2AlC. The surface energies of M(C)-terminated surfaces are therefore increased because of larger energy difference between M–Al d–p bonding orbitals and M–M d–d metallic bonding orbitals when Ti is substituted by V and Cr.

4. Conclusion

Stable M_2AlC (M = Ti, V and Cr) (0001) surfaces were studied using density functional theory calculations. Four

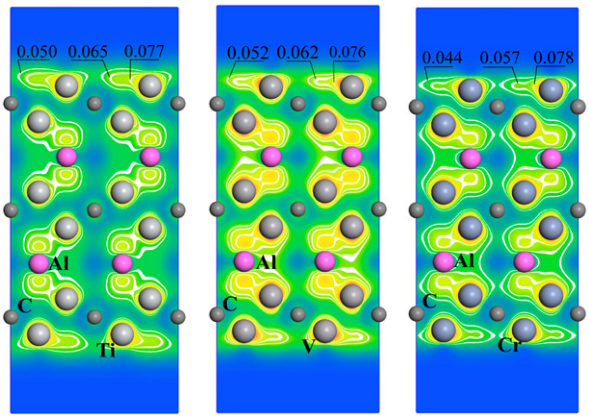

Figure 7. Valence electron density of M(C)-terminated (0001) surfaces. The plots are in the (1120) plane. Panel (a) includes the energy range between −2.40 and 0.73 eV in Ti_2AlC. Panel (b) covers from −3.18 to −0.02 eV in V_2AlC. Panel (c) ranges from −3.55 to −0.52 eV in Cr_2AlC.

possible surfaces were considered. Based on the calculated surface energies, Al- and M(C)-terminated (0001) surfaces are more stable than C- and M(Al)-terminated surfaces. The stability of M_2AlC(0001) surfaces under different chemical environments was also analyzed. Precipitation of some related binary carbides was considered during the analysis. The results show that, for Ti_2AlC and V_2AlC, both the Al- and M(C)-terminated surfaces can be stable under different chemical conditions; while for Cr_2AlC, only the Al- terminated surface is stable. For Al-terminated surfaces of M_2AlC, only Ti_2AlC experiences strengthening of the Ti–Al bond in the surface area; while the other two compounds suffer increased surface energies from occupying M–Al antibonding states in the surface area. In turn, for the M(C)-terminated surface, the redistributed 3d electrons prefer to occupy the M–M d–d metallic bonding states. The surface energies of M(C)-terminated surfaces get larger because of the larger energy difference between M–Al d–p bonding orbitals and M–M d–d metallic bonding orbitals from Ti_2AlC to V_2AlC and Cr_2AlC.

Acknowledgments

This work was supported by the National Outstanding Young Scientist Foundation for Y C Zhou under grant no. 59925208, and the Natural Sciences Foundation of China under grant nos 50672102, 90403027 and 50302011.

References

[1] Barsoum M W 2000 *Prog. Solid State Chem.* **28** 201
[2] Raucault C, Langlais F, Naslain R and Kihn Y 1994 *J. Mater. Res.* **29** 3941
[3] Palmquist J P, Li S, Persson P O A, Emmerlich J, Wilhelmsson O, Högberg H, Katsnelsson M, Johansson B, Ahuja R, Eriksson O, Hultman L and Jansson U 2004 *Phys. Rev.* B. **70** 165401
[4] Emmerlich J, Palmquist J P, Högberg H, Molina-Aldareguia J M, Czigány Zs, Sasvàri Sz, Person P, Jansson U and Hultman L 2004 *J. Appl. Phys.* **96** 4817
[5] Gulbiński W, Gilewicz A, Suszko T, Warcholiński B and Kukliński Z 2004 *Surf. Coat. Technol.* **180/181** 341
[6] Palmquist J P, Jansson U, Seppänen T, Persson P O A, Birch J, Hultman L and Isberg P 2002 *Appl. Phys. Lett.* **81** 835
[7] Högberg H, Hultman L, Emmerlich J, Joelsson T, Eklund P, Molina-Aldareguia J M, Palmquist J P, Wilhelmsson O and Jansson U 2005 *Surf. Coat. Technol.* **193** 6
[8] Wilhelmsson O, Palmquist J P, Nyberg T and Jansson U 2004 *Appl. Phys. Lett.* **85** 1066
[9] Wilhelmsson O, Palmquist J P, Lewin E, Emmerlich J, Eklund P, Persson P O A, Högberg H, Li S, Ahuja R, Eriksson O, Hultman L and Jansson U 2006 *J. Cryst. Growth* **291** 290
[10] Schneider J M, Sun Z, Mertens R, Uestel F and Ahuja R 2004 *Solid State Commun.* **130** 445
[11] Mertens R, Sun Z, Music D and Schneider J M 2004 *Adv. Eng. Mater.* **6** 903
[12] Walter C, Sigumonrong D P, El-Raghy T and Schneider J M 2006 *Thin Solid Films* **515** 389
[13] Sun Z and Ahuja R 2006 *Appl. Phys. Lett.* **88** 161913
[14] Music D, Sun Z, Ahuja R and Schneider J M 2006 *J. Phys.: Condens. Matter* **18** 8877
[15] Music D, Sun Z, Ahuja R and Schneider J M 2007 *Surf. Sci.* **601** 896
[16] Zhang H Z and Wang S Q 2007 *Acta. Mater.* **55** 4645
[17] Wang X H and Zhou Y C 2003 *Oxid. Met.* **59** 303
[18] Lin Z J, Zhou Y C, Li M S and Wang J Y 2005 *Z. Metallkd.* **96** 291
[19] Segall M D, Lindan P L D, Probert M J, Pickard C J, Hasnip P J, Clark S J and Payne M C 2002 *J. Phys.: Condens. Matter* **14** 2717
[20] Vanderbilt D 1990 *Phys. Rev.* B **41** 7892
[21] Perdew J P, Chevary J A, Vosko S H, Jackson K A, Perderson M R, Singh D J and Fiolhais C 1992 *Phys. Rev.* B **46** 6671
[22] Mattson A E and Jennison D R 2002 *Surf. Sci. Lett.* **520** L611
[23] Yu D and Scheffler M 2004 *Phys. Rev.* B **70** 155417
[24] Jiang D E and Cater E A 2005 *Acta. Mater.* **53** 4489
[25] Siegel D J, Hector L G and Adams J B 2002 *Phys. Rev.* B **65** 085415
[26] Ho J, Heifets E and Merinov B 2007 *Surf. Sci.* **601** 490
[27] Reuter K and Scheffler M 2001 *Phys. Rev.* B **65** 035406
[28] Wang X G, Weiss W, Shaikhutdinov Sh K, Ritter M, Petersen M, Wagner F, Schlögl R and Scheffler M 1998 *Phys. Rev. Lett.* **81** 1038
[29] Smith J R and Zhang W 2000 *Acta. Mater.* **48** 4395
[30] Zhang W and Smith J R 2000 *Phys. Rev.* B **61** 16883
[31] Feng J W, Zhang W Q, Jiang W and Gu H 2006 *Phys. Rev. Lett.* **97** 246102
[32] Monkhorst H J and Pack J D 1977 *Phys. Rev.* B **16** 1748
[33] Fischer T H and Almlof J 1992 *J. Phys. Chem.* **96** 9768
[34] Wang J Y, Zhou Y C, Liao T and Lin Z J 2006 *Appl. Phys. Lett.* **89** 021917
[35] Liao T, Wang J Y and Zhou Y C 2006 *Phys. Rev.* B **77** 174112
[36] Wang J Y, Zhou Y C, Lin Z J, Liao T and He L F 2006 *Phys. Rev.* B **73** 134107
[37] Wang J Y, Zhou Y C and Lin Z J 2005 *Appl. Phys. Lett.* **87** 051902
[38] Liu B, Wang J Y, Zhou Y C, Liao T and Li F Z 2007 *Acta. Mater.* **55** 2949
[39] Wang J Y, Zhou Y C and Lin Z J 2007 *Acta. Mater.* **55** 6019
[40] Heifets E, Eglitis R I, Kotomin E A, Maier J and Borstel G 2001 *Phys. Rev.* B **64** 76
[41] Kotomin E A, Eglitis R I, Maier J and Heifets E 2001 *Thin Solid Films* **400** 76
[42] Bottin F, Finocchi F and Noguera C 2003 *Phys. Rev.* B **68** 035418

[43] Qian G X, Martin R M and Chadi D J 1988 *Phys. Rev.* B **38** 7649
[44] Wang X G, Chaka A and Scheffler M 2000 *Phys. Rev. Lett.* **84** 3650
[45] Johnston K, Castell M R, Paxton A T and Finnis M W 2004 *Phys. Rev.* B **70** 085415
[46] Padilla J and Vanderbilt D 1997 *Phys. Rev.* B **56** 1625
[47] Ahuja R, Eriksson O, Wills J M and Johnansson B 2000 *Appl. Phys. Lett.* **76** 2226
[48] Sun Z, Ahuja R, Li S and Schneider J M 2003 *Appl. Phys. Lett.* **83** 899
[49] Wang J Y and Zhou Y C 2004 *Phys. Rev.* B **69** 214111
[50] Wang J Y and Zhou Y C 2004 *J. Phys.: Condens. Matter* **16** 2819